ESC HEART FAILURE
ESC Heart Failure 2019; **6**: 1015–1026
Published online 19 July 2019 in Wiley Online Library (wileyonlinelibrary.com) **DOI:** 10.1002/ehf2.12497

ORIGINAL RESEARCH ARTICLE

Assessing the role of extracellular signal-regulated kinases 1 and 2 in volume overload-induced cardiac remodelling

Svenja Jochmann[1†], Manar Elkenani[1,2†], Belal A. Mohamed[1,3,7], Eric Buchholz[1,3], Dawid Lbik[1,3], Lutz Binder[3,4], Kristina Lorenz[5,6], Ajay M. Shah[2], Gerd Hasenfuß[1,3], Karl Toischer[1,3] and Moritz Schnelle[1,3,4*]

[1]*Department of Cardiology and Pneumology, University Medical Center Göttingen, Göttingen, Germany;* [2]*King's College London British Heart Foundation Centre of Excellence, School of Cardiovascular Medicine & Sciences, London, UK;* [3]*DZHK (German Centre for Cardiovascular Research), Partner Site Göttingen, Göttingen, Germany;* [4]*Institute for Clinical Chemistry, University Medical Center Göttingen, Robert-Koch-Str. 40, 37075 Göttingen, Germany;* [5]*Institute of Pharmacology and Toxicology, Würzburg, Germany;* [6]*Leibniz-Institut für Analytische Wissenschaften—ISAS e.V., Dortmund, Germany;* [7]*Department of Medical Biochemistry and Molecular Biology, Mansoura Faculty of Medicine, Mansoura, Egypt*

Abstract

Aims Volume overload (VO) and pressure overload (PO) induce differential cardiac remodelling responses including distinct signalling pathways. Extracellular signal-regulated kinases 1 and 2 (ERK1/2), key signalling components in the mitogen-activated protein kinase (MAPK) pathways, modulate cardiac remodelling during pressure overload (PO). This study aimed to assess their role in VO-induced cardiac remodelling as this was unknown.

Methods and results Aortocaval fistula (Shunt) surgery was performed in mice to induce cardiac VO. Two weeks of Shunt caused a significant reduction of cardiac ERK1/2 activation in wild type (WT) mice as indicated by decreased phosphorylation of the TEY (Thr-Glu-Tyr) motif (−28% as compared with Sham controls, $P < 0.05$). Phosphorylation of other MAPKs was unaffected. For further assessment, transgenic mice with cardiomyocyte-specific ERK2 overexpression (ERK2tg) were studied. At baseline, cardiac ERK1/2 phosphorylation in ERK2tg mice remained unchanged compared with WT littermates, and no overt cardiac phenotype was observed; however, cardiac expression of the atrial natriuretic peptide was increased on messenger RNA (3.6-fold, $P < 0.05$) and protein level (3.1-fold, $P < 0.05$). Following Shunt, left ventricular dilation and hypertrophy were similar in ERK2tg mice and WT littermates. Left ventricular function was maintained, and changes in gene expression indicated reactivation of the foetal gene program in both genotypes. No differences in cardiac fibrosis and kinase activation was found amongst all experimental groups, whereas apoptosis was similarly increased through Shunt in ERK2tg and WT mice.

Conclusions VO-induced eccentric hypertrophy is associated with reduced cardiac ERK1/2 activation *in vivo*. Cardiomyocyte-specific overexpression of ERK2, however, does not alter cardiac remodelling during VO. Future studies need to define the pathophysiological relevance of decreased ERK1/2 signalling during VO.

Keywords ERK1/2; Volume overload; Aortocaval fistula model; Cardiac remodelling; Eccentric hypertrophy

Received: 8 April 2019; Revised: 29 May 2019; Accepted: 18 June 2019
**Correspondence to: Moritz Schnelle, Institute for Clinical Chemistry, University Medical Center Göttingen, Robert-Koch-Str. 40, 37075 Göttingen, Germany. Tel: +49 5513965510; Fax : +49 551397038. Email: moritz.schnelle@med.uni-goettingen.de*
†Equal contribution

Introduction

Heart failure (HF) development and progression are associated with alterations in cardiac gene expression as well as molecular, cellular, and interstitial changes in the heart causing differences in cardiac shape, size, and function.[1] The term *cardiac remodelling* encompasses all of these changes. Based on shape and size, three different patterns of left ventricular (LV) remodelling can be distinguished: concentric remodelling (increased wall thickness but normal mass), concentric hypertrophy (increased wall thickness and mass), and eccentric hypertrophy (increased dimensions

and mass).[2] In various cardiovascular diseases, these distinctive LV remodelling responses can be induced through haemodynamic stress, that is, pressure overload (PO) and volume overload (VO).[3] Hypertension or aortic stenosis are typically associated with PO causing concentric LV remodelling and hypertrophy, respectively. Initially, this response is compensatory as it reduces wall stress according to the law of Laplace. Diseases like aortic and mitral regurgitation, in contrast, primarily lead to VO causing eccentric hypertrophy. From a haemodynamic point of view, this response can be considered maladaptive due to an increase in wall stress. A murine study, however, demonstrated a more favourable cardiac phenotype following VO compared with PO.[4] This included a longer preservation of systolic function, less adverse LV remodelling, and a better survival. These different phenotypes could be attributed at least partially to differences in cardiac signalling mechanisms following VO and PO. A detailed and better understanding of such mechanisms driving LV remodelling is needed for novel therapeutic strategies to target HF.[5]

In this context, the mitogen-activated protein kinases (MAPKs) have been shown to be pivotal signalling molecules involved in cardiac remodelling and cardiovascular diseases in response to different stimuli.[6] The MAPK signalling cascade typically involves activation through MAPK kinases (MKKs; e.g. MEK1/2), which are themselves phosphorylated and thereby activated by MKK kinases (MKKKs; e.g. Raf-1). Three main branches of MAPKs are distinguished, involving p38 kinases, c-Jun N-terminal kinases (JNKs), and extracellular signal-regulated kinases 1/2 (ERK1/2).[7] Once phosphorylated, MAPKs become activated and regulate a diverse range of intracellular targets affecting important regulatory events including growth, differentiation, and survival. With respect to cardiac remodelling and hypertrophy, particularly ERK1/2 signalling has been shown to be of great importance.[8,9] However, contradictory findings from murine studies hamper a clear understanding of its precise role.[6] Canonical ERK1/2 activation is mediated by MEK1/2-dependent phosphorylation in the TEY (Thr-Glu-Tyr) motif of their activation loops.[10] Bueno *et al*.[11] showed that cardiomyocyte-specific MEK1 overexpression and subsequent ERK1/2 activation cause a physiological form of concentric hypertrophy with enhanced systolic function and improved resistance to apoptotic stimuli. In accordance with these findings, specific deletion of ERK2 in cardiomyocytes was shown to attenuate PO-induced cardiac hypertrophy in mice.[12] In contrast, a different study reported increased cardiac hypertrophy with pronounced systolic dysfunction following PO in mice with a cardiomyocyte-specific ERK2 deletion.[13] Targeted ERK1/2 inactivation in the heart through overexpression of the dual-specificity phosphatase 6 (DUSP6) was shown to not diminish cardiac growth in response to both pathological and physiological stimuli, suggesting that ERK1/2 signalling is not required for cardiac hypertrophy.[14] These controversial findings highlight the need for a more comprehensive understanding of how ERK1/2 precisely affects cardiac remodelling.

The aim of this study was to assess a potential involvement of ERK1/2 in cardiac remodelling during VO as this has not yet been investigated. Therefore, VO was induced through aortocaval fistula (Shunt) surgery in wild type (WT) and transgenic mice with cardiomyocyte-specific ERK2 overexpression (ERK2tg) followed by subsequent morphological, functional, and molecular analyses.

Materials and methods

Mice

The investigation conforms to the *Guide for the Care and Use of Laboratory Animals* published by the US National Institutes of Health (publication no. 85-23, revised 1985). All animal work was approved by the responsible agency (Niedersächsisches Landesamt für Verbraucherschutz und Lebensmittelsicherheit) and was performed in accordance with the institutional guidelines.

For pure WT experiments, C57Bl/6N mice aged 8–10 weeks were purchased from Charles River (Sulzfeld, Germany). Transgenic mice from the FVB/N background expressing ERK2 under the control of the mouse α-*myosin heavy chain* promoter and WT littermates were generated as previously described (named $Erk2^{T188T}$ in the study by Lorenz *et al*.).[9] For our experiments, they were crossed into the C57Bl/6J strain for more than 10 generations, and only male and age-matched animals were used.

Aortocaval fistula (Shunt)

The aortocaval fistula (Shunt) model was used to induce VO in mice as described previously.[4] Mice undergoing this procedure were at least 10 weeks of age, and the surgeries were performed under 1.5% isoflurane. Briefly, a longitudinal abdominal incision was made, the intestine was put aside, and the aorta as well as the inferior vena cava were dissected free from any surrounding tissue. The aorta was clamped just above the renal arteries and punctured with a 23-gauge needle passing through to the inferior vena cava in an infrarenal position. The lateral aortic puncture site was then sealed with cyanoacrylate glue. The abdomen was closed, and the mice were kept on a heating plate until full recovery from anaesthesia. Sham animals underwent the same procedure except for vessel puncture. Mice were studied 2 weeks post-surgery.

Heart weight measurements

Mice were sacrificed under 5% isoflurane by cervical dislocation. To expose the beating heart, the ribcage was opened

and removed. Then, both atria and ventricles were dissected free, dried, and weighed using a fine balance (Sartorius, Germany). The respective tibia length (TL) of each animal was used for normalization.

Echocardiography

Mice were anesthetized with 1.5% isoflurane, and transthoracic echocardiography was performed in a supine position using a Vevo 2100 Imaging System (Visualsonics, Canada). During this procedure, the core temperature was maintained at 37 °C, and heart rates were kept consistent between experimental groups at 400–500 b.p.m. Electrocardiogram monitoring was obtained using hind limb electrodes. LV geometry and systolic function were assessed by using standard 2D parasternal long and short axis views. As previously described, speckle tracking was performed to quantify the peak longitudinal strain rate during early LV filling [termed reverse longitudinal strain rate (rLSR)] for assessment of diastolic function.[15] The examiner was blinded towards group assignment.

Quantitative real-time polymerase chain reaction

DNA-free RNA was extracted from LV tissue with the RNeasy kit and the RNase-free DNAse Set (Qiagen, Germany), followed by cDNA synthesis using the iScript cDNA synthesis kit (Bio-Rad Laboratories, Germany) according to manufacturer's instructions. Gene expression was assessed via quantitative real-time polymerase chain reaction on a Bio-Rad iQ-Cycler. Transcripts of interest were amplified and measured using SYBR green fluorescent dye. Relative gene expression was calculated with the delta-delta Ct method using GAPDH as denominator. The following primer sequences were used:

GAPDH (*Gapdh*)	Sense:	GAGACGGCCGCATCTTCTT
	Antisense:	CAATCTCCACTTTGCCACTGC
ANP (*Nppa*)	Sense:	GGGGGTAGGATTGACAGGAT
	Antisense:	CAGAATCGACTGCCTTTTCC
BNP (*Nppb*)	Sense:	ACAAGATAGACCGGATCGGA
	Antisense:	ACCCAGGCAGAGTCAGAAAC
SERCA-2α (*Atp2a2*)	Sense:	GGGCAAAGTGTATCGACAGG
	Antisense:	TCAGCAGGAACTTTGTCACC
α-Skeletal actin (*Acta1*)	Sense:	CTCACTTCCTACCCTCGGC
	Antisense:	GCCGTTGTCACACACAAGAG

Histology

LV tissue was harvested, fixed in 4% buffered formaldehyde overnight, paraffin embedded, sectioned (5 μm), and stained with fluorescein-conjugated wheat germ agglutinin (WGA-Alexa Fluor 594; Invitrogen, USA) for cross-sectional area (CSA) assessment. At least 400 randomly selected cardiomyocytes per animal were measured using the Image J software (Bethesda, USA). Picrosirius red (Abcam, UK) staining for evaluation of fibrosis was performed according to standard procedure. At least two randomly selected sections per LV were analysed and quantified with the Image J software. TdT-mediated dUTP-biotin nick end labelling (TUNEL) staining for detection of apoptotic cells was performed using the In Situ Cell Death Detection Kit (Roche, Germany) according to the manufacturer's instructions. TUNEL-positive cells were counted in five to eight random fields (20×) per LV.

Western blot analysis

Snap-frozen LV tissue was homogenized in RIPA buffer (Merck Millipore, USA) containing protease and phosphatase inhibitor cocktails (Roche). Protein concentration was measured using Pierce BCA Protein Assay (Thermo Fisher Scientific, USA). Tissue homogenates containing 20 μg of protein were then separated by sodium dodecyl sulphate-polyacrylamide gel electrophoresis (SDS-PAGE) and transferred onto nitrocellulose membranes (Bio-Rad Laboratories). The following primary antibodies were used: anti-phospho-Akt (Ser473), anti-total Akt, anti-phospho-ERK1/2 (Thr202/Tyr204), anti-total ERK1/2, anti-phospho-p38 (Thr180/Tyr182), anti-total p38, anti-phospho-JNK (Thr183/Tyr185), anti-total JNK (all from Cell Signaling, USA), anti-phospho-ERK1/2 Thr188 (Badrilla, UK), anti-ANP N-terminal (Abcam), anti-SERCA-2α (Thermo Fisher Scientific), and anti-GAPDH (Merck Millipore). Membranes were subsequently incubated with horseradish peroxidase-conjugated secondary antibodies (anti-rabbit from Cell Signaling and anti-mouse from GE Healthcare, UK) followed by detection of protein bands using an enhanced chemiluminescent detection system (GE Healthcare) according to the manufacturer's instructions. For quantification, band intensity was measured using the Image Lab software (Bio-Rad).

Statistical analysis

Data are presented as mean ± SEM. Unpaired Student's *t*-tests and two-way ANOVA followed by Bonferroni test for multiple comparisons were used where appropriate. $P < 0.05$ was considered statistically significant. All statistical analyses were performed using GraphPad Prism v7 (San Diego, USA).

Results

Reduced cardiac ERK1/2 activation during VO-induced eccentric hypertrophy

Following 2 weeks of cardiac VO through aortocaval fistula (Shunt) surgery, eccentric LV hypertrophy was confirmed via

post-mortem morphometric analysis and echocardiography in WT C57Bl/6 mice. Shunt induced LV hypertrophy and dilation with significant increases in LV weight/tibia length (LV/TL) ratio and left ventricular end-diastolic diameter (LVEDD) without affecting the septal wall thickness as compared with Sham controls (*Figure 1A–C*). This pattern of cardiac remodelling was associated with a significant decrease in ERK1/2 phosphorylation of the TEY motif (−28%, $P < 0.05$; *Figure 1D*) indicating reduced canonical ERK1/2 activation in the heart. In addition to TEY phosphorylation, activation of ERK1/2 through autophosphorylation at Thr188 was shown to be an important mechanism as it directs ERK1/2 to nuclear targets causing cardiac hypertrophy.[9] However, phosphorylation of Thr188 in LV lysates was unaffected in the Shunt group (*Figure 1D*) and so were phosphorylation levels of other MAPKs, i.e. JNK and p38 (*Figure 1E*).

Baseline characterization of cardiomyocyte-specific ERK2 transgenic mice in the C57Bl/6 background

Cardiac characterization of ERK2 transgenic (ERK2tg) mice in the C57Bl/6 background was carried out at baseline first before subjecting them to Shunt. As shown in the FVB/N background, ERK2tg mice were viable and developed normally. Protein expression of ERK2 was increased by 10.5-fold in hearts of ERK2tg mice compared with WT littermates,

Figure 1 Assessment of eccentric LV hypertrophy and cardiac MAPK activation levels in WT mice following 2 weeks of VO. (A–C) LV weight to tibia length ratio (LV/TL), left ventricular end-diastolic diameter (LVEDD), and septal wall thickness (Septum) were assessed in WT mice through post-mortem morphometric analysis (LV/TL) and echocardiography (LVEDD, Septum) 2 weeks after Shunt and Sham control surgery. (D, E) Cardiac phosphorylation levels of ERK1/2 (of both TEY motif and the autophosphorylated Thr188) (D), JNK and p38 (E) were evaluated by Western blotting. Band intensities were normalized to the respective total protein for quantification and GAPDH served as loading control.
* $P < 0.05$, ** $P < 0.01$, n.s. not significant using unpaired Student's *t*-test. Numbers in bars reflect the number of mice.

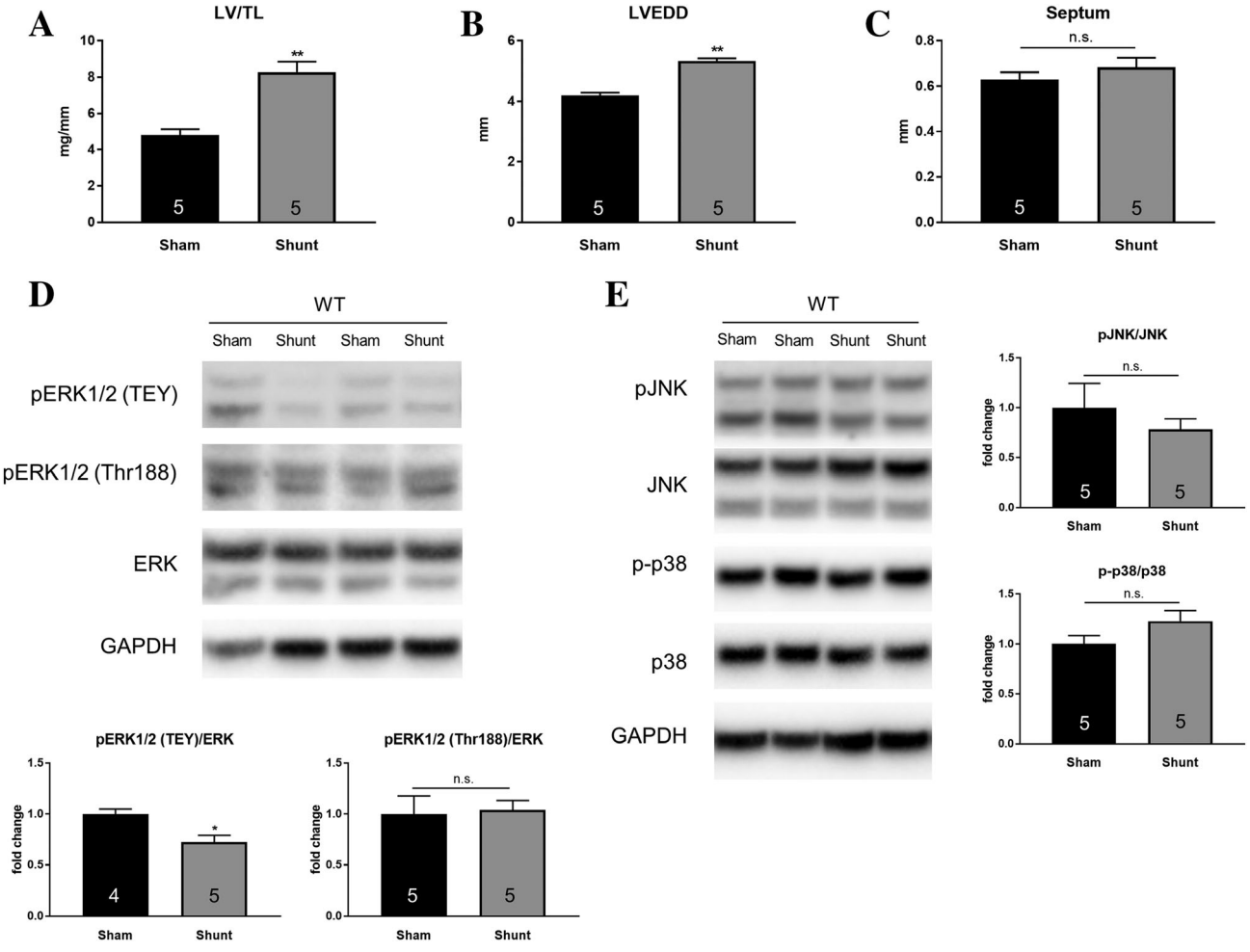

whereas ERK1 levels were unchanged (*Figure 2A*). The overexpression of ERK2 was not associated with altered ERK1/2 phosphorylation of both the TEY motif and the autophosphorylation site at Thr188 (*Figure 2A*). Echocardiography revealed no differences in LV geometry (assessed via LVEDD and septum thickness) and systolic function (assessed via ejection fraction) between ERK2tg mice and WT littermates (*Figure 2B–E*). The LV mass was also comparable, as the LV/TL ratio did not differ (*Figure 2F*).

Molecular characterization of cardiac stress markers showed a markedly increased expression of natriuretic peptide type A (*Nppa*, ANP) on both mRNA and protein level in LV lysates from ERK2tg mice compared with WT littermates (*Figure 3A, B*). This regulation appeared to be specific for ANP as gene expression of other stress markers, for example, natriuretic peptide TYPE B (*Nppb*, BNP) and α-skeletal actin (*Acta1*) were unchanged (*Figure 3A*). Sarcoplasmic/endoplasmic reticulum calcium ATPase-2α (*Atp2a2*, SERCA-2α) was significantly reduced on cardiac mRNA but not protein level in ERK2tg mice (*Figure 3A, B*).

VO-induced cardiac remodelling is not affected by cardiomyocyte ERK2 overexpression

Following 2 weeks of Shunt, echocardiography was performed in ERK2tg mice and WT littermates to assess LV geometry and function. Representative M-mode images are shown in *Figure 4A*. Comparable increases in LVEDD indicated similar levels of LV dilation in both genotypes compared with Sham controls (*Figure 4B*, *Table 1*). Septal wall thickness, heart rate, systolic function via assessment of the ejection fraction, and the rLSR as readout for diastolic function were not different amongst all experimental groups (*Figure 4C–F*, *Table 1*). Compared with the respective Sham

Figure 2 Baseline cardiac characterization of ERK2tg mice. (A) Expression levels of total ERK2 protein and ERK1/2 phosphorylation (of both the TEY motif and the autophosphorylated Thr188) were assessed in LV lysates from ERK2tg mice and WT littermates by Western blotting. Band intensities were normalized to GAPDH for quantification. (B) Representative M-mode echocardiographic images. (C–F). Measurements of LVEDD, septum thickness, ejection fraction, and LV/TL ratio. ** $P < 0.01$, n.s. not significant using unpaired Student's *t*-test. Numbers in (or above) bars reflect the number of mice. LVEDD, left ventricular end-diastolic diameter; LV/TL, LV weight to tibia length ratio.

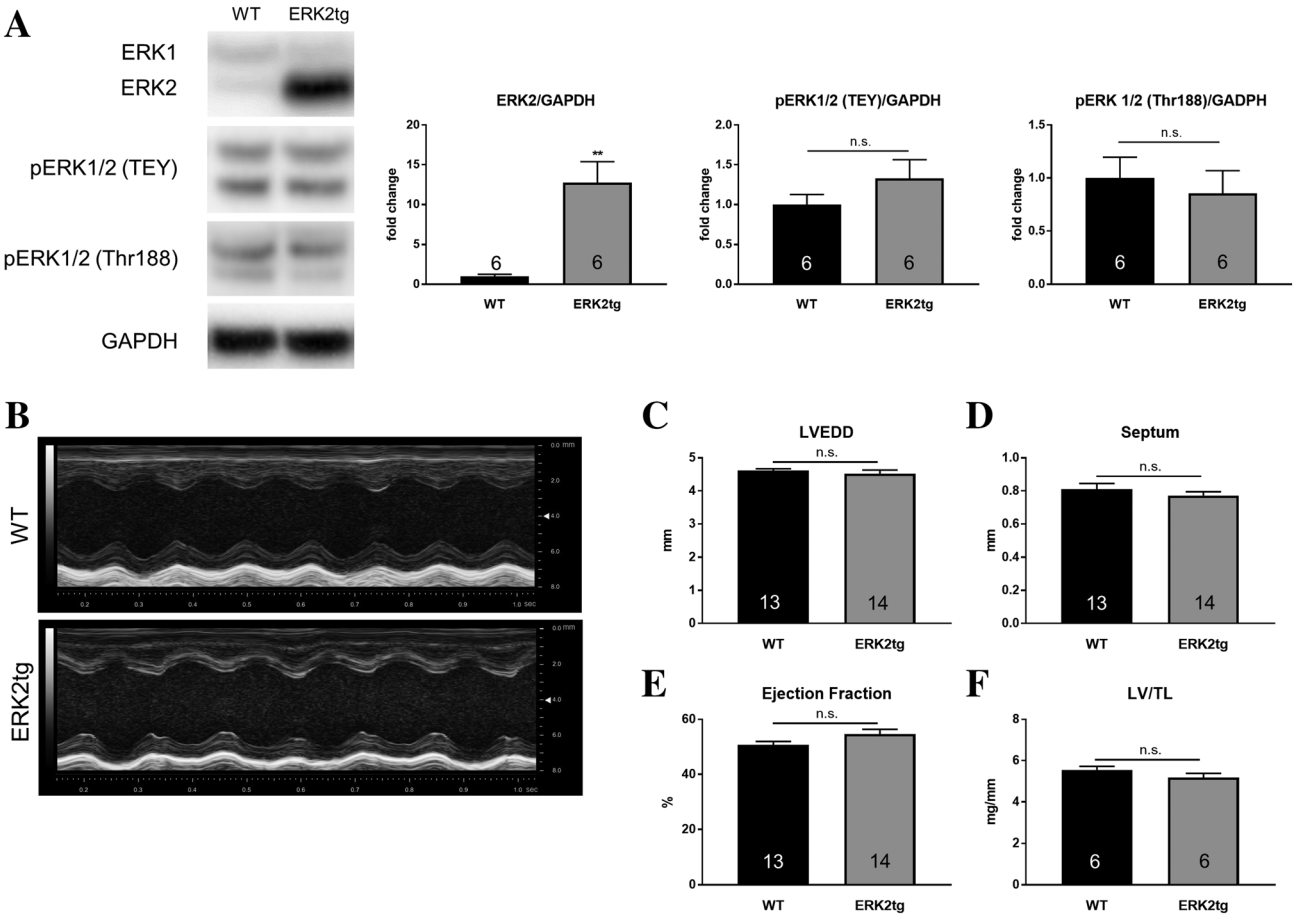

DOI: 10.1002/ehf2.12497

Figure 3 Gene expression of cardiac stress markers in ERK2tg mice at baseline. (A) Gene expression of ANP (*Nppa*), BNP (*Nppb*) α-skeletal actin (*Acta1*), and SERCA-2α (*Atp2a2*) in LV lysates from ERK2tg mice compared with WT littermates was assessed using quantitative real-time polymerase chain reaction. GAPDH served as denominator. (B) Protein expression of ANP and SERCA-2α was assessed by Western blotting. Band intensities were normalized to GAPDH for quantification. * $P < 0.05$, ** $P < 0.01$, n.s. not significant using unpaired Student's *t*-test. Numbers in bars reflect the number of mice.

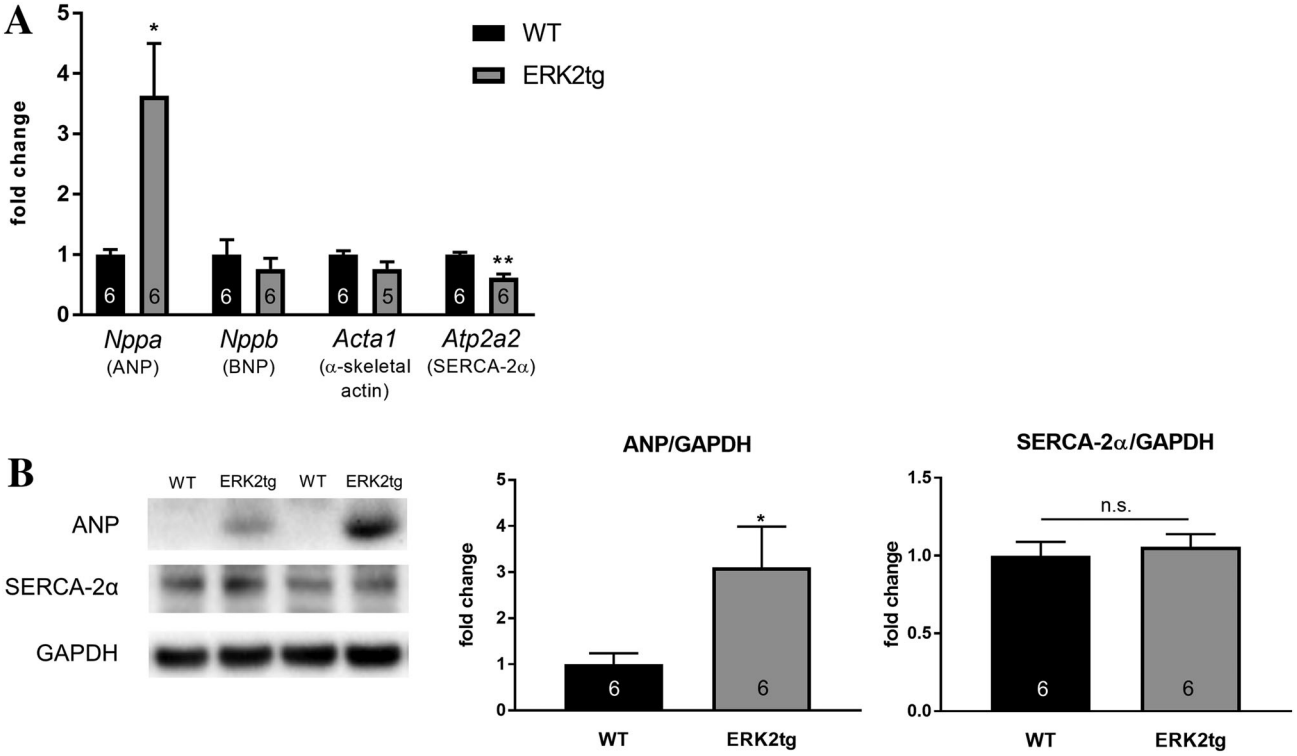

group, the increase in LV/TL (WT: +38%, $P < 0.01$; ERK2tg: +31%, $P < 0.05$) ratio revealed similar levels of LV hypertrophy in both genotypes following Shunt, although there was a statistically non-significant tendency towards less hypertrophy in ERK2tg mice (*Figure 4G*, *Table 1*). These findings indicate similar LV geometry and function in ERK2tg mice and WT littermates following Shunt.

For further characterization of cardiac remodelling, histological analyses were performed in LV sections after 2 weeks of Shunt. Cross sectional area (CSA) measurements demonstrated small increases in cardiomyocyte size through Shunt, which did not reach statistical significance and were comparable between WT and ERK2tg mice (*Figure 5A, B*). Cardiac fibrosis was analysed via Picrosirius red staining and displayed no differences amongst all four experimental groups (*Figure 5A, C*). TUNEL positive cells were significantly increased following Shunt indicating induction of apoptosis; however, to a similar degree in both ERK2tg and WT mice (*Figure 5A, D*).

Shunt also induced similar trends with respect to gene expression of cardiac stress markers in WT and ERK2tg mice, that is, increased ANP, BNP, and α-skeletal actin and decreased SERCA-2α levels (*Table 2*). Although not consistently significant, these changes indicate a return to the foetal gene program in both genotypes.

As shown for WT mice, cardiac ERK1/2 TEY phosphorylation was also significantly reduced in ERK2tg mice following Shunt (*Figure 6A*). Phosphorylation of other relevant kinases in the heart, such as Akt, JNK, and p38 remained unchanged in both WT and ERK2tg mice indicating unchanged activation levels (*Figure 6B*).

Discussion

VO and PO induce distinctive signalling mechanisms in the heart driving differential cardiac remodelling, that is, eccentric and concentric hypertrophy. This explains why therapeutic efficacy of certain drugs, for example, angiotensin converting enzyme inhibitors, varies depending on the disease pathophysiology and related mechanisms.[16] PO, for instance, is associated with early activation of calcium/calmodulin-dependent protein kinase II (CaMKII) in the heart and detrimental downstream effects, whereas the

Figure 4 LV geometry, function, and hypertrophy in ERK2tg mice following VO. (A) Representative M-mode echocardiographic images from ERK2tg mice and WT littermates 2 weeks after Shunt and Sham. (B–F) LVEDD, septum thickness, heart rate, ejection fraction, and reverse longitudinal strain rate (rLSR) were assessed using echocardiography. (G) LV/TL ratio. * $P < 0.05$ and ** $P < 0.01$ vs. corresponding Sham, n.s. not significant between genotypes using two-way ANOVA with Bonferroni post-test. Numbers in bars reflect the number of mice. LVEDD, left ventricular end-diastolic diameter; LV/TL, LV weight to tibia length ratio.

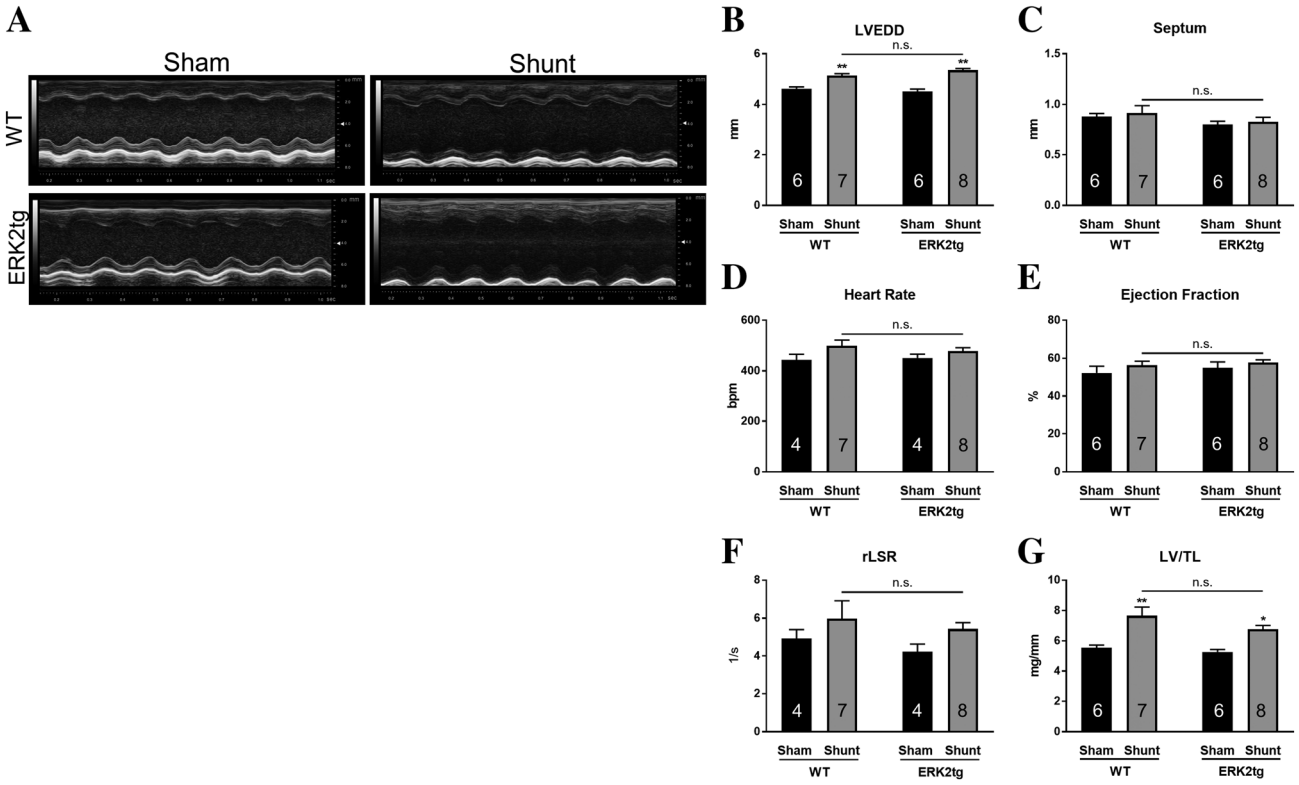

same duration of VO induces beneficial activation of protein kinase B (Akt) without altering CaMKII phosphorylation levels.[4] The majority of studies performed in animal models in this context focus on PO and concentric hypertrophy; thus, a better understanding of relevant mechanisms in the heart during VO-induced eccentric hypertrophy is needed.

Kehat *et al*.[13] demonstrated previously that loss of ERK1/2 signalling in mice causes cardiomyocyte lengthening, i.e. eccentric hypertrophy. We tested whether this applies vice versa, i.e. whether eccentric hypertrophy is associated with reduced cardiac ERK1/2 activation *in vivo*. Thus, WT mice were subjected to 2 weeks of VO via Shunt surgery to induce eccentric hypertrophy. Subsequent molecular analyses revealed that cardiac ERK1/2 activation through phosphorylation of the TEY motif indeed decreased significantly as compared with Sham controls. Phosphorylation levels of other MAPKs, that is, JNK and p38, remained unaffected. To our knowledge, this is the first *in vivo* cardiac stress model resulting in decreased cardiac ERK1/2 activation. The majority of studies consistently report augmented ERK1/2 activation upon different cardiac stimuli including biomechanical stress and neurohormonal factors.[17] Whether cardiac ERK1/2 is activated or deactivated therefore appears to be dependent on the particular stimulus. It could be speculated that the reduced cardiac ERK1/2 phosphorylation during VO is due to a stretch-induced increase in specific phosphatase activity. In line with this hypothesis, a recent study carried out in rat isolated papillary muscles showed that stretch can induce expression of DUSP6.[18] In our *in vivo* model of VO, phosphatases like DUSP6 could potentially be activated by a preload-mediated stretch of proteins involved in preload sensing such as the giant molecule titin. This, however, needs further evaluation. It is noteworthy that other groups did not report any differences in ERK1/2 phosphorylation in the heart following VO.[4,19] This could be due to differences in the experimental design: (i) the study by Toischer *et al*. was carried out in FVB/N mice, whereas we used mice from C57Bl/6 background; (ii) the duration of VO was shorter, that is, 1 week instead of 2 weeks in our study; (iii) You *et al*. used a novel murine model of aortic regurgitation to induce VO, which most likely differed in severity compared with our well-established aortocaval fistula (Shunt) model.[20] As ERK1/2 activation is transient and depends, amongst other factors, on the duration and strength of a given stimulus,[21] the

DOI: 10.1002/ehf2.12497

Table 1 Echocardiographic and morphometric measurements in ERK2tg mice and WT littermates 2 weeks after Shunt and Sham procedure

	WT		ERK2tg	
	Sham	Shunt	Sham	Shunt
Number of mice	6	7	6	8
Echocardiography				
Heart rate (b.p.m.)	444 ± 23	500 ± 23	452 ± 15	479 ± 13
LVEDD (mm)	4.63 ± 0.07	5.15 ± 0.08[b]	4.51 ± 0.10	5.35 ± 0.07[b]
LVESD (mm)	3.37 ± 0.12	3.66 ± 0.13	3.17 ± 0.13	3.66 ± 0.09[a]
EF (%)	52.3 ± 3.5	56.4 ± 2.1	55.0 ± 3.0	57.8 ± 1.5
FS (%)	26.1 ± 1.6	29.8 ± 1.4	28.6 ± 2.0	30.8 ± 1.0
SV (μL)	50.1 ± 1.6	71.7 ± 1.5[b]	50.6 ± 2.6	79.5 ± 2.3[b]
Septum (mm)	0.88 ± 0.03	0.92 ± 0.07	0.80 ± 0.03	0.83 ± 0.04
PW (mm)	0.83 ± 0.04	0.86 ± 0.07	0.72 ± 0.02	0.73 ± 0.02
rLSR (1/s)	4.92 ± 0.48	5.97 ± 0.96	4.22 ± 0.41	5.43 ± 0.33
Morphometry				
BW (g)	30.5 ± 0.8	31.5 ± 0.6	32.0 ± 0.8	30.5 ± 0.8
HW/TL (mg/mm)	7.41 ± 0.16	10.80 ± 0.93[b]	6.87 ± 0.28	9.47 ± 0.32[a]
LV/TL (mg/mm)	5.55 ± 0.17	7.67 ± 0.58[b]	5.18 ± 0.20	6.78 ± 0.24[a]
RV/TL (mg/mm)	1.42 ± 0.04	1.79 ± 0.15	1.21 ± 0.09	2.0 ± 0.11[b]

BW, body weight; EF, ejection fraction; FS, fractional shortening; HW/TL, heart weight to tibia length ratio; LVEDD, left ventricular end-diastolic diameter; LVESD, left ventricular end-systolic diameter; LV/TL, left ventricular weight to tibia length ratio; PW, posterior wall thickness during diastole; rLSR, reverse longitudinal strain rate; RV/TL, right ventricular weight to tibia length ratio; Septum, septal thickness during diastole; SV, stroke volume. The following *P* values denote between Shunt and respective Sham controls using two-way ANOVA with Bonferroni post-test:
[a]*$p<0.05$, **$p<0.01$ between Shunt and respective Sham controls using two-way ANOVA with Bonferroni post-test.
[b]* $p<0.05$, ** $p<0.01$ between Shunt and respective Sham controls using unpaired Student's t-test.

discrepant findings regarding cardiac ERK1/2 activation during VO can at least be partially attributed to different methodological approaches.

In addition to phosphorylation of the TEY motif, an alternative pathway of ERK2 activation involving autophosphorylation on Thr188 has been introduced by Lorenz *et al.*[9] in 2009. More recently, this particular mode of ERK2 activation was shown to contribute to adverse cardiac remodelling in response to pathological stimuli but did not interfere with physiological hypertrophy during voluntary exercise in mice.[22] In our model of eccentric hypertrophy, cardiac Thr188 phosphorylation remained unaffected. This fits the concept that short-term VO-induced eccentric hypertrophy reflects a rather physiological form of cardiac remodelling with beneficial signalling and the absence of cardiac dysfunction.[23]

Compared with ERK1, ERK2 contributes significantly more to the protein content of total ERK1/2 in the heart.[24] Thus, the role of ERK2 alone is of particular interest with respect to cardiac remodelling and hypertrophy.[25] Given the fact that VO, according to our findings, is associated with a decrease in cardiac ERK activation, we hypothesized that overexpression of ERK2 in cardiomyocytes would affect cardiac remodelling in the context of VO-induced eccentric hypertrophy. Firstly, previously generated ERK2tg mice (FVB/N background)[9] were crossed into a C57Bl/6 background to be consistent regarding genetic strains throughout our experiments. It is important to mention that we have used two different C57Bl/6 substrains in our study (i.e. C57Bl/6N for pure WT experiments and C57Bl/6J for generation of ERK2tg mice and WT littermates). Previous experiments from our laboratory demonstrate that C57Bl/6N and C57Bl/6J do not differ with respect to their cardiac response to 2 weeks of Shunt including comparable morphological changes and a similar reduction of ERK1/2 phosphorylation (data not shown); thus, using different C57Bl/6 substrains was unlikely to affect the results of this study. Baseline characterization of the newly generated ERK2tg mice revealed no overt cardiac phenotype compared with WT littermates. LV morphology and function, as assessed via echocardiography, were similar and no differences in heart weights were observed. Despite a 10.5-fold increase in cardiac ERK2 protein content, phosphorylation of the TEY motif in ERK2tg mice remained unaffected as compared with WT littermates. This is in accordance with previous observations showing that ERK2 activity is limited by upstream signals rather than its expression levels.[9] Unexpectedly, cardiomyocyte ERK2 overexpression at baseline induced the expression of ANP on both mRNA and protein level in the heart. Expression of other cardiac stress markers, such as BNP, α-skeletal actin and SERCA-2α were either unchanged or differed only on mRNA level (e.g. SERCA-2α). Thus, ERK2 can distinctively regulate ANP expression in the heart independent from its activation status. This seems to be a unique feature in the C57Bl/6 background as it has not been described before. Given the important role of ANP in cardiac remodelling and HF progression,[26,27] further studies are needed to identify the precise molecular mechanisms underlying this novel regulation and its pathophysiological relevance. Apart from the difference in baseline cardiac ANP expression and well-known mouse

Figure 5 Cardiomyocyte hypertrophy, LV fibrosis, and apoptosis in ERK2tg mice following VO. (A). Representative histological images from transverse LV sections of ERK2tg mice and WT littermates following 2 weeks of Shunt and Sham. Cross sectional area (CSA) was assessed via wheat germ agglutinin (WGA) staining, fibrosis was detected through Picrosirius red staining and apoptosis via TUNEL assay (white arrow indicates TUNEL-positive cells). (B–D) Quantification of CSA (per cardiomyocyte), fibrosis (% area), and apoptosis (number of TUNEL-positive cells per 10^5 nuclei identified via DAPI staining). * $P < 0.05$ and ** $P < 0.01$ vs. corresponding Sham, n.s. not significant between genotypes using two-way ANOVA with Bonferroni post-test. Numbers in bars reflect the number of mice.

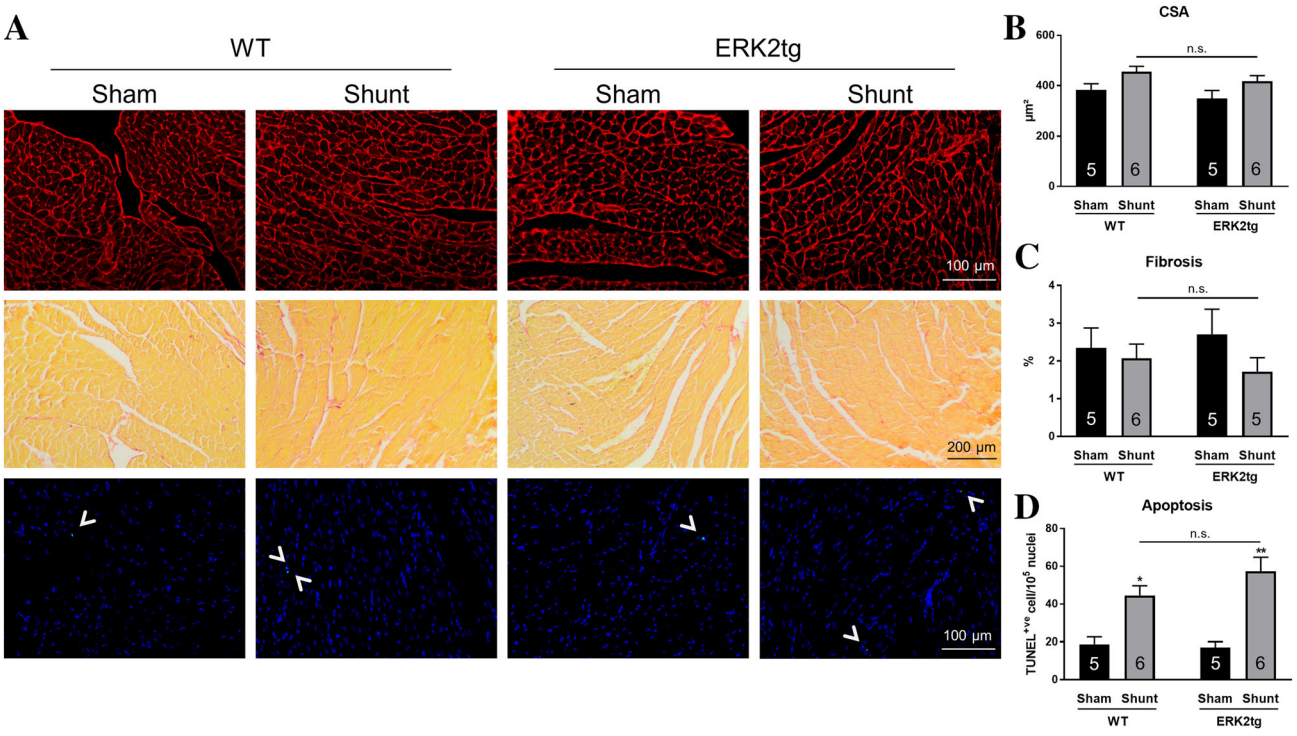

strain-specific features, for example, higher baseline contractility in FVB/N compared with C57Bl/6 mice,[28] ERK2tg mice and WT littermates used in this study (C57Bl/6 background) showed no relevant baseline difference compared with the mice used by Lorenz *et al*. (FVB/N background).

Similar to WT, 2 weeks of VO caused significantly decreased cardiac ERK1/2 activation levels in ERK2tg mice as compared with Sham controls. Against our hypothesis, levels of LV dilation and hypertrophy were comparable between ERK2tg and WT littermates following Shunt. In both genotypes, changes in gene expression of cardiac stress markers following Shunt were indicative of a reactivation of the foetal gene program in cardiomyocytes, a typical hallmark during cardiac stress.[29] Systolic and diastolic function were assessed via echocardiography, remained unchanged between both genotypes, and did not differ between Sham and Shunt groups. The latter was expected as the Shunt model is associated with a long period of cardiac compensation until HF develops.[4,30] As our study was carried out at only one time point 2 weeks after Shunt, this does not rule out the possibility that increased ERK2 abundance might affect LV geometry and function following long term VO. The similar responses in both genotypes might be due to the lack of increased ERK2 activation in ERK2tg mice, which limits the impact of our findings.

Table 2 Gene expression profiles of cardiac stress markers in ERK2tg mice and wild type littermates 2 weeks after Shunt

	WT	ERK2tg
ANP	2.46 ± 0.80	2.00 ± 0.27*
BNP	1.99 ± 0.32*	2.17 ± 0.27**
α-Skeletal actin	3.48 ± 1.17	1.94 ± 0.30*
SERCA-2α	0.61 ± 0.04**	0.83 ± 0.08

ANP (*Nppa*), BNP (*Nppb*), α-skeletal actin (*Acta1*), and SERCA-2α (*Atp2a2*) mRNA levels were assessed in LV lysates via quantitative real-time polymerase chain reaction, and GAPDH was used as denominator. Fold changes vs. respective Sham group are shown; n = 5–8/group. The following P values denote between Shunt and respective Sham controls using unpaired Student's t-test:
*$P < 0.05$.
**$P < 0.01$.

ERK1/2 signalling plays an important role in the development of cardiac fibrosis and apoptosis during PO.[9,12] Our histological analyses revealed that cardiomyocyte-specific overexpression of ERK2 did not affect the levels of fibrosis and apoptosis in the heart following 2 weeks of VO. Whereas fibrosis remained unchanged amongst all groups, apoptosis

Figure 6 Kinase phosphorylation in ERK2tg mice following VO. (A) ERK1/2 phosphorylation of the TEY motif was assessed in LV lysates from ERK2tg mice after 2 weeks of Shunt and Sham by Western blotting. Band intensities were normalized to total ERK for quantification. (B) Phosphorylation of Akt, JNK, and p38 in ERK2tg mice and WT littermates following Shunt and Sham. Band intensities were normalized to total levels of respective kinases for quantification. GAPDH was used as loading control. * $P < 0.05$ using unpaired Student's *t*-test (A), n.s. not significant between genotypes using two-way ANOVA with Bonferroni post-test (B). Numbers in bars reflect the number of mice.

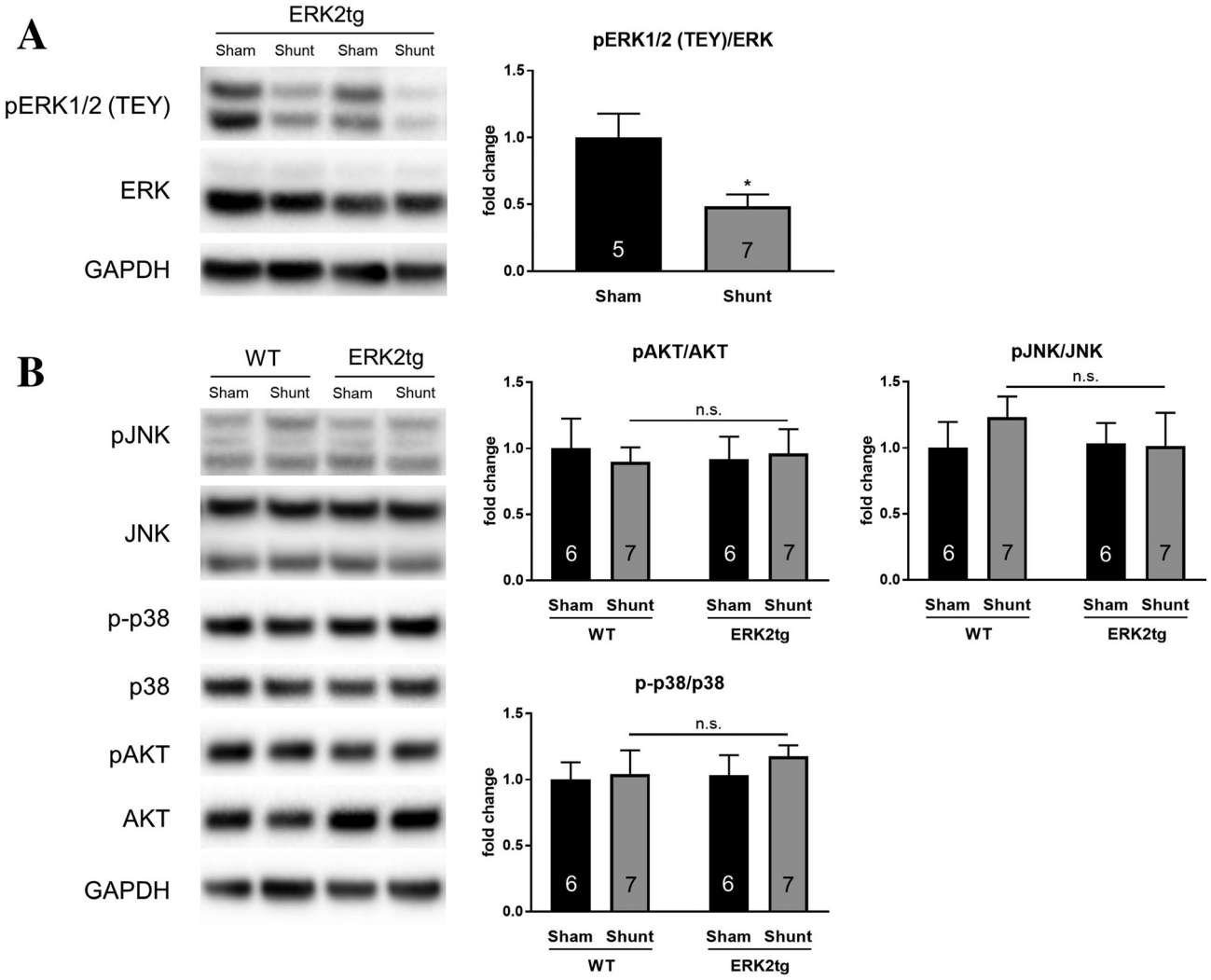

as early pathological feature during experimental VO[4,19] was significantly increased, but to a similar degree in both genotypes following Shunt.

Akt activation was previously shown to be an important cardiac signalling mechanism during VO as it promotes eccentric hypertrophy to handle the increased volume.[31] Accordingly, Akt-deficient mice displayed less eccentric hypertrophy following VO, which was associated with earlier deterioration of systolic function and higher mortality as compared with WT littermates.[30] However, as HF progresses during chronic VO, the initial Akt activation in the heart decreases. Our study was most likely carried out in the transition phase between early activation and late deactivation of Akt, which is why cardiac phosphorylation levels appeared unchanged after Shunt even in WT mice.

In conclusion, we show for the first time that VO-induced eccentric hypertrophy is associated with a reduction in cardiac ERK1/2 activation *in vivo*. Cardiomyocyte-specific overexpression of ERK2 was not sufficient to affect cardiac remodelling in response to VO. This may be due to the fact that ERK2 overexpression did not induce ERK2 activation in the heart; however, as shown for PO, activation is required for ERK2 to modulate cardiac remodelling.[9,32] As this is a limitation of the current study, subjecting mice with increased ERK1/2 activity (e.g. through alteration of specific phosphatase activity) to Shunt would be an interesting approach to get a better

understanding of how ERK1/2 is involved in VO-induced eccentric hypertrophy.

Conflict of interest

None declared.

Funding

This work was supported by the Deutsche Forschungsgemeinschaft (DFG) (IRTG1816 to S.J., M.E., and M.S. and SFB1002 to G.H. and K.T.). Further funding was provided by the Federal Ministry of Education and Research (BMBF) (to K.L.) and the German Centre for Cardiovascular Research (DZHK).

References

1. Cohn JN, Ferrari R, Sharpe N. Cardiac remodeling—concepts and clinical implications: a consensus paper from an international forum on cardiac remodeling. Behalf of an International Forum on Cardiac Remodeling. *J Am Coll Cardiol* 2000; **35**: 569–582.
2. Ganau A, Devereux RB, Roman MJ, de Simone G, Pickering TG, Saba PS, Vargiu P, Simongini I, Laragh JH. Patterns of left ventricular hypertrophy and geometric remodeling in essential hypertension. *J Am Coll Cardiol* 1992; **19**: 1550–1558.
3. Grossman W, Jones D, McLaurin LP. Wall stress and patterns of hypertrophy in the human left ventricle. *J Clin Invest* 1975; **56**: 56–64.
4. Toischer K, Rokita AG, Unsold B, Zhu W, Kararigas G, Sossalla S, Reuter SP, Becker A, Teucher N, Seidler T, Grebe C, Preuss L, Gupta SN, Schmidt K, Lehnart SE, Kruger M, Linke WA, Backs J, Regitz-Zagrosek V, Schafer K, Field LJ, Maier LS, Hasenfuss G. Differential cardiac remodeling in preload versus afterload. *Circulation* 2010; **122**: 993–1003.
5. Xie M, Burchfield JS, Hill JA. Pathological ventricular remodeling: therapies: part 2 of 2. *Circulation* 2013; **128**: 1021–1030.
6. Rose BA, Force T, Wang Y. Mitogen-activated protein kinase signaling in the heart: angels versus demons in a heartbreaking tale. *Physiol Rev* 2010; **90**: 1507–1546.
7. Garrington TP, Johnson GL. Organization and regulation of mitogen-activated protein kinase signaling pathways. *Curr Opin Cell Biol* 1999; **11**: 211–218.
8. Mutlak M, Kehat I. Extracellular signal-regulated kinases 1/2 as regulators of cardiac hypertrophy. *Front Pharmacol* 2015; **6**: 149.
9. Lorenz K, Schmitt JP, Schmitteckert EM, Lohse MJ. A new type of ERK1/2 autophosphorylation causes cardiac hypertrophy. *Nat Med* 2009; **15**: 75–83.
10. Shaul YD, Seger R. The MEK/ERK cascade: from signaling specificity to diverse functions. *Biochim Biophys Acta* 2007; **1773**: 1213–1226.
11. Bueno OF, De Windt LJ, Tymitz KM, Witt SA, Kimball TR, Klevitsky R, Hewett TE, Jones SP, Lefer DJ, Peng CF, Kitsis RN, Molkentin JD. The MEK1-ERK1/2 signaling pathway promotes compensated cardiac hypertrophy in transgenic mice. *EMBO J* 2000; **19**: 6341–6350.
12. Ulm S, Liu W, Zi M, Tsui H, Chowdhury SK, Endo S, Satoh Y, Prehar S, Wang R, Cartwright EJ, Wang X. Targeted deletion of ERK2 in cardiomyocytes attenuates hypertrophic response but provokes pathological stress induced cardiac dysfunction. *J Mol Cell Cardiol* 2014; **72**: 104–116.
13. Kehat I, Davis J, Tiburcy M, Accornero F, Saba-El-Leil MK, Maillet M, York AJ, Lorenz JN, Zimmermann WH, Meloche S, Molkentin JD. Extracellular signal-regulated kinases 1 and 2 regulate the balance between eccentric and concentric cardiac growth. *Circ Res* 2011; **108**: 176–183.
14. Purcell NH, Wilkins BJ, York A, Saba-El-Leil MK, Meloche S, Robbins J, Molkentin JD. Genetic inhibition of cardiac ERK1/2 promotes stress-induced apoptosis and heart failure but has no effect on hypertrophy in vivo. *Proc Natl Acad Sci U S A* 2007; **104**: 14074–14079.
15. Schnelle M, Catibog N, Zhang M, Nabeebaccus AA, Anderson G, Richards DA, Sawyer G, Zhang X, Toischer K, Hasenfuss G, Monaghan MJ, Shah AM. Echocardiographic evaluation of diastolic function in mouse models of heart disease. *J Mol Cell Cardiol* 2018; **114**: 20–28.
16. Chandrashekhar Y. Embracing diversity in remodeling: a step in therapeutic decision making in heart failure? *J Am Coll Cardiol* 2007; **49**: 822–825.
17. Lorenz K, Schmitt JP, Vidal M, Lohse MJ. Cardiac hypertrophy: targeting Raf/MEK/ERK1/2-signaling. *Int J Biochem Cell Biol* 2009; **41**: 2351–2355.
18. Zavala MR, Diaz RG, Medina AJ, Acosta MP, Escudero DS, Ennis IL, Perez NG, Villa-Abrille MC. p38-MAP kinase negatively regulates the slow force response to stretch in rat myocardium through the up-regulation of dual specificity phosphatase 6 (DUSP6). *Cell Physiol Biochem* 2019; **52**: 172–185.
19. You J, Wu J, Zhang Q, Ye Y, Wang S, Huang J, Liu H, Wang X, Zhang W, Bu L, Li J, Lin L, Ge J, Zou Y. Differential cardiac hypertrophy and signaling pathways in pressure versus volume overload. *Am J Physiol Heart Circ Physiol* 2018; **314**: H552–H562.
20. Scheuermann-Freestone M, Freestone NS, Langenickel T, Hohnel K, Dietz R, Willenbrock R. A new model of congestive heart failure in the mouse due to chronic volume overload. *Eur J Heart Fail* 2001; **3**: 535–543.
21. Kehat I, Molkentin JD. Extracellular signal-regulated kinase 1/2 (ERK1/2) signaling in cardiac hypertrophy. *Ann N Y Acad Sci* 2010; **1188**: 96–102.
22. Ruppert C, Deiss K, Herrmann S, Vidal M, Oezkur M, Gorski A, Weidemann F, Lohse MJ, Lorenz K. Interference with ERK (Thr188) phosphorylation impairs pathological but not physiological cardiac hypertrophy. *Proc Natl Acad Sci U S A* 2013; **110**: 7440–7445.
23. Olsen NT, Dimaano VL, Fritz-Hansen T, Sogaard P, Chakir K, Eskesen K, Steenbergen C, Kass DA, Abraham TP. Hypertrophy signaling pathways in experimental chronic aortic regurgitation. *J Cardiovasc Transl Res* 2013; **6**: 852–860.
24. Lips DJ, Bueno OF, Wilkins BJ, Purcell NH, Kaiser RA, Lorenz JN, Voisin L, Saba-El-Leil MK, Meloche S, Pouyssegur J, Pages G, De Windt LJ, Doevendans PA, Molkentin JD. MEK1-ERK2 signaling pathway protects myocardium from ischemic injury in vivo. *Circulation* 2004; **109**: 1938–1941.
25. Del Re DP, Sadoshima J. Elucidating ERK2 function in the heart. *J Mol Cell Cardiol* 2014; **72**: 336–338.
26. Wang D, Gladysheva IP, Fan TH, Sullivan R, Houng AK, Reed GL. Atrial natriuretic peptide affects cardiac remodeling, function, heart failure, and survival in a mouse model of dilated cardiomyopathy. *Hypertension* 2014; **63**: 514–519.
27. Mori T, Chen YF, Feng JA, Hayashi T, Oparil S, Perry GJ. Volume overload results in exaggerated cardiac hypertrophy in the atrial natriuretic peptide knockout mouse. *Cardiovasc Res* 2004; **61**: 771–779.
28. Shah AP, Siedlecka U, Gandhi A, Navaratnarajah M, Al-Saud SA, Yacoub

MH, Terracciano CM. Genetic background affects function and intracellular calcium regulation of mouse hearts. *Cardiovasc Res* 2010; **87**: 683–693.
29. Taegtmeyer H, Sen S, Vela D. Return to the fetal gene program: a suggested metabolic link to gene expression in the heart. *Ann N Y Acad Sci* 2010; **1188**: 191–198.
30. Mohamed BA, Schnelle M, Khadjeh S, Lbik D, Herwig M, Linke WA, Hasenfuss G, Toischer K. Molecular and structural transition mechanisms in long-term volume overload. *Eur J Heart Fail* 2016; **18**: 362–371.
31. Ikeda M, Ide T, Fujino T, Matsuo Y, Arai S, Saku K, Kakino T, Oga Y, Nishizaki A, Sunagawa K. The Akt-mTOR axis is a pivotal regulator of eccentric hypertrophy during volume overload. *Sci Rep* 2015; **5**: 15881.
32. Bueno OF, Molkentin JD. Involvement of extracellular signal-regulated kinases 1/2 in cardiac hypertrophy and cell death. *Circ Res* 2002; **91**: 776–781.